J Elast
https://doi.org/10.1007/s10659-018-9672-7

Free Damage Propagation with Memory

Robert Lipton[1] · **Eyad Said**[1] · **Prashant Jha**[1]

Received: 15 July 2017

Abstract We introduce a simple model for free damage propagation based on non-local potentials. The model is developed using a state based peridynamic formulation. The resulting evolution is shown to be well posed. At each instant of the evolution we identify the damage set. On this set the local strain has exceeded critical values either for tensile or hydrostatic strain and damage has occurred. For this model the damage set is nondecreasing with time and associated with damage variables defined at each point in the body. We show that energy balance holds for this evolution. For differentiable displacements away from the damage set we show that the nonlocal model converges to the linear elastic model.

Keywords Nonlocal model · Damage · Memory · Peridynamics

Mathematics Subject Classification 74R05 · 74R10

1 Introduction

We address the problem of damage propagation in materials. The damage evolution is not known a-priori and is found as part of the problem solution. Our approach is to use a nonlocal formulation with a minimum number of parameters describing the model. We will work within the small deformation setting and the model is developed within a state based peridynamic formulation. Here strains are expressed in terms of displacement differences as opposed to spatial derivatives. For the problem at hand the non-locality provides the flexibility to simultaneously model non-differentiable displacements and damage evolution. The net force acting on a point x is due to the strain between x and neighboring points y. The

This material is based upon work supported by the U.S. Army Research Laboratory and the U.S. Army Research Office under contract/grant number W911NF1610456.

✉ R. Lipton
lipton.robert@gmail.com

[1] Department of Mathematics and Center for Computation and Technology, Louisiana State University, Baton Rouge, LA 70803, USA

Published online: 14 March 2018

neighborhood of nonlocal interaction between x and its neighbors y is confined to ball of radius δ centered at x denoted by $B_\delta(x)$. The radius of the ball is called the called the horizon. Numerical implementations based on nonlocal peridynamic models exhibit formation and localization of features associated with phase transformation and fracture see for example [1–3, 8–10, 14, 21, 23–25]. A recent review can be found in [4].

The recent model studied in [11–14] is defined by double well two point strain potentials. Here one potential well is centered at the origin and associated with elastic response while the other well is at infinity and associated with surface energy. The rational for studying these models is that they are shown to be well posed and, in the limit of vanishing nonlocality, the dynamics recovers features associated with sharp fracture propagation see, [12] and [13]. While memory is not incorporated in this model it is seen that the inertia of the evolution keeps the forces in a softened state over time as evidenced in simulations [14]. This modeling approach is promising for fast cracks but for cyclic loading and slowly propagating fractures an explicit damage-fracture modeling with memory is needed. In this work we develop this approach for general models that allow for three point nonlocal interactions and irreversible damage. The use of three point potentials allows one to model a larger variety of elastic properties. In the lexicon of peridynamics we adopt an ordinary state based formulation [18, 22]. We introduce non-local forces that soften irreversibly as the shear strain or dilatational strain increases beyond critical values. This model is shown to deliver a mathematically well posed evolution. Here the existence and uniqueness of the evolution is guaranteed by the Lipschitz continuity of the nonlocal force. The Lipschitz constant blows up to infinity as inertial forces go to zero, see (3.23). This asymptotic loss of continuity is consistent with a loss of uniqueness for the quasi-static limit. The existence of instability and non-uniqueness is well known for quasi-static gradient damage models [17].

Previous work establishes existence and uniqueness for peridynamic bond based evolutions with bond breaking for small [6] and large [5] deformations. In addition to being state based our modeling approach is distinct from other investigations [5, 6, 19] and uses differentiable damage variables. This feature allows us to establish an energy balance equation relating kinetic energy, potential energy, and energy dissipation at each instant during the evolution. At each instant we identify the set undergoing damage where the local energy dissipation rate is positive. On this set the local strain has exceeded a critical value and damage has occurred. Damage is irreversible and the damage set is monotonically increasing with time. Explicit damage models are illustrated and force strain curves for both cyclic loading and strain to failure are provided. We show theoretically that the nonlocal operator converges to the linear local operator associated with the elastic wave equation away from the damage set. In this limit the elastic tensor can have any combination of Poison ratio and Young's modulus. This result is consistent with small horizon convergence results for convex energies, see [7, 15, 23] and convex-concave energies [11–13]. We provide numerical simulations demonstrating the effects of damage evolution by this model. The loss of stiffness due to damage is illustrated for a three and four point bending problem as well as the cyclic decrease of stiffness and the associated hysteresis for an oscillatory boundary load. These simulations agree with the trends presented in [26].

2 Formulation

We assume the displacements u are small (infinitesimal) relative to the size of the three dimensional body D. The tensile strain is written as $S = S(y, x, t; u)$ and given by

$$S(y, x, t; u) = \frac{u(t, y) - u(t, x)}{|y - x|} \cdot e_{y-x}, \quad e_{y-x} = \frac{y - x}{|y - x|}, \tag{2.1}$$

where e_{y-x} is a unit direction vector and $\cdot$ is the dot product. It is evident that $S(y,x,t;u)$ is the tensile strain along the direction e_{y-x}. We introduce the nonnegative weight $\omega^\delta(|y-x|)$ such that $\omega^\delta = 0$ for $|y-x| > \delta$ and the spherical or hydrostatic strain at x is given by

$$\theta(x,t;u) = \frac{1}{V_\delta}\int_{D\cap B_\delta(x)} \omega^\delta(|y-x|)|y-x|S(y,x,t;u)\,dy, \tag{2.2}$$

where V_δ is the volume of the ball $B_\delta(x)$ of radius δ centered at x. The weight is chosen such that $\omega^\delta(|y-x|) = \omega(|y-x|/\delta)$, and

$$\ell_1 = \frac{1}{V_\delta}\int_{B_\delta(x)} \omega^\delta(|y-x|)\,dy < \infty. \tag{2.3}$$

We follow [18] and [6] and introduce a nonnegative damage factor taking the value one in the undamaged region and zero in the fully damaged region. The damage factor for the force associated with tensile strains is written $H^T(u)(y,x,t)$, the corresponding factor for hydrostatic strains is written $H^D(u)(x,t)$. Here we assume no damage and $H^T(u)(y,x,t) = 1$ until a critical tensile strain S_c is reached. For tensile strains greater than S_c damage is initiated and $H^T(u)(y,x,t)$ drops below 1. The fully damaged state is $H^T(u)(y,x,t) = 0$. For hydrostatic strains we assume no damage until a critical positive dilatational strain θ_c^+ or a negative compressive strain (θ_c^-) is reached. Again $H^D(u)(x,t) = 1$ until a critical hydrostatic strain is reached and then drops below 1 with the fully damaged state being $H^D(u)(x,t) = 0$. We postpone description of the specific form of the history dependent damage factors until after we have defined the nonlocal forces.

The force at a point x due to tensile strain is given by

$$\mathcal{L}^T(u)(x,t) = \frac{2}{V_\delta}\int_{D\cap B_\delta(x)} \frac{J^\delta(|y-x|)}{\delta|y-x|} H^T(u)(y,x,t)\partial_S f\big(\sqrt{|y-x|}S(y,x,t;u)\big)e_{y-x}\,dy, \tag{2.4}$$

Here $J^\delta(|y-x|)$ is a nonnegative bounded function such that $J^\delta = 0$ for $|y-x| > \delta$ and $M = \sup\{y \in B_\delta(x);\, J^\delta(|y-x|)\}$ and

$$\ell_2 = \frac{1}{V_\delta}\int_{B_\delta(x)} \frac{J^\delta(|y-x|)}{|y-x|^2}\,dy < \infty \quad \text{and} \quad \ell_3 = \frac{1}{V_\delta}\int_{B_\delta(x)} \frac{J^\delta(|y-x|)}{|y-x|^{3/2}}\,dy < \infty. \tag{2.5}$$

Both J^δ and ω^δ are prescribed and characterize the influence of nonlocal forces on x by neighboring points y. Here ∂_S is the partial derivative with respect to strain. The function $f = f(r)$ is twice differentiable for all arguments r on the real line and f', f'' are bounded. Here we take $f(r) = \alpha r^2/2$ for $r < r_1$ and $f = r$ for $r_2 < r$, with $r_1 < r_2$, see Fig. 1. The factor $\sqrt{|y-x|}$ appearing in the argument of $\partial_S f$ ensures that the nonlocal operator $\mathcal{L}^T$ converges to the divergence of a stress tensor in the small horizon limit when its known a-priori that displacements are smooth, see Sect. 7.

The force at a point x due to the hydrostatic strain is given by

$$\mathcal{L}^D(u)(x,t) = \frac{1}{V_\delta}\int_{D\cap B_\delta(x)} \frac{\omega^\delta(|y-x|)}{\delta^2}\big[H^D(u)(y,t)\partial_\theta g\big(\theta(y,t;u)\big) \tag{2.6}$$

$$+ H^D(u)(x,t)\partial_\theta g\big(\theta(x,t;u)\big)\big]e_{y-x}\,dy, \tag{2.7}$$

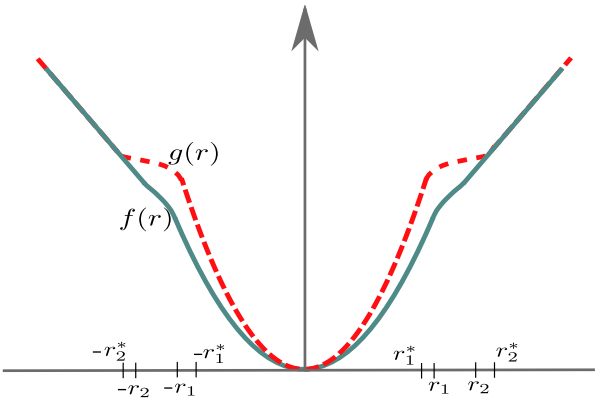

Fig. 1 Generic plot of $f(r)$ (solid line) and $g(r)$ (dashed line)

where the function $g(r) = \beta r^2/2$ for $r < r_1^*$, $g = r$ for $r_2^* < r$, with $r_1^* < r_2^*$ and g is twice differentiable and g', g'' are bounded, see Fig. 1. It is readily verified that the force $\mathcal{L}^T(u)(x,t) + \mathcal{L}^D(u)(x,t)$ satisfies balance of linear and angular momentum.

The damage factor for tensile strain $H^T(u)(y,x,t)$ is given in terms of the functions $h(x)$ and $j_S(x)$. Here h is nonnegative, has bounded derivatives (hence Lipschitz continuous), takes the value one for negative x and for $x \geq 0$ decreases and is zero for $x > x_c$, see Fig. 2. Here we are free to choose x_c to be any small and positive number. The function $j_S(x)$ is nonnegative, has bounded derivatives (hence Lipschitz continuous), takes the value zero up to a positive critical strain S_C and then takes on positive values. We will suppose $j_S(x) \leq \gamma|x|$ for some $\gamma > 0$, see Fig. 3. The damage factor is now defined to be

$$H^T(u)(y,x,t) = h\left(\int_0^t j_S\big(S(y,x,\tau;u)\big)\,d\tau\right). \tag{2.8}$$

It is clear from this definition that damage occurs when the strain exceeds S_c for some period of time and the bond force decreases irrevocably from its undamaged value. The damage function defined here is symmetric, i.e., $H^T(u)(y,x,t) = H^T(u)(x,y,t)$. For hydrostatic strain we introduce the nonnegative function j_θ with bounded derivatives (hence Lipschitz continuous). We suppose $j_\theta = 0$ for an interval containing the origin given by (θ_c^-, θ_c^+) and takes positive values outside this interval, see Fig. 4. As before we will suppose $j_\theta(x) \leq \gamma|x|$ for some $\gamma > 0$, the damage factor for hydrostatic strain is given by

$$H^D(u)(x,t) = h\left(\int_0^t j_\theta\big(\theta(x,\tau;u)\big)\,d\tau\right). \tag{2.9}$$

For this model it is clear that damage can occur irreversibly for compressive or dilatational strain when the possibly different critical values θ_c^- or θ_c^+ are exceeded.

The *damage set* at time t is defined to be the collection of all points x for which $H^T(u)(y,x,t)$ or $H^D(u)(x,t)$ is less than one. This set is monotonically increasing in time. The *process zone* at time t are the collection of points x undergoing damage such that $\partial_t H^T(u)(y,x,t) > 0$ or $\partial_t H^D(u)(x,t) > 0$. Explicit examples of $H^T(u)(y,x,t)$ and $H^D(u)(x,t)$ are given in Sect. 5.

We define the body force $b(x,t)$ and the displacement $u(x,t)$ is the solution of the initial value problem given by

$$\rho\partial_t^2 u(x,t) = \mathcal{L}^T(u)(x,t) + \mathcal{L}^D(u)(x,t) + b(x,t) \quad \text{for } x \in D \text{ and } t \in (0,T), \tag{2.10}$$

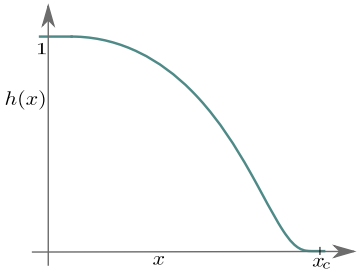

Fig. 2 Generic plot of $h(x)$

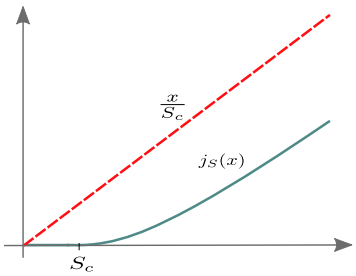

Fig. 3 Generic plot of $j_S(x)$ with S_c

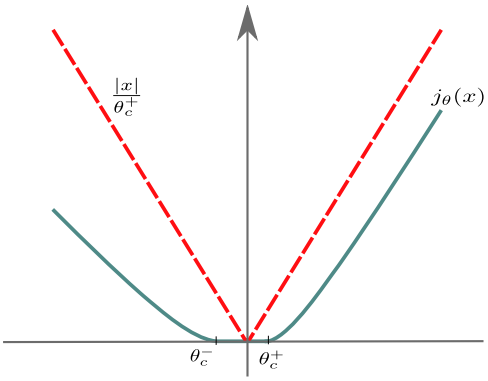

Fig. 4 Generic plot of $j_\theta(x)$ with θ_c^+, and θ_c^-

with initial data

$$u(x,0) = u_0(x), \qquad \partial_t u(x,0) = v_0(x). \tag{2.11}$$

It is easily verified that this is an ordinary state based peridynamic model. We show in the next section that this initial value problem is well posed.

3 Existence of Solutions

The regularity and existence of the solution depends on the regularity of the initial data and body force. In this work we choose a general class of body forces and initial conditions. The initial displacement u_0 and velocity v_0 are chosen to be integrable and bounded and belonging to $L^\infty(D;\mathbb{R}^3)$. The space of such functions is denoted by $L^\infty(D;\mathbb{R}^3)$ The body force $b(x,t)$ is chosen such that for every $t \in [0,T_0]$, b takes values in $L^\infty(D,\mathbb{R}^3)$

and is continuous in time. The associated norm is defined to be $\|b\|_{C([0,T_0];L^\infty(D,\mathbb{R}^3))} = max_{t\in[0,T_0]}\|b(x,t)\|_{L^\infty(D,\mathbb{R}^3)}$. The associated space of continuous functions in time taking values in $L^\infty(D;\mathbb{R}^3)$ for which this norm is finite is denoted by $C([0,T_0];L^\infty(D,\mathbb{R}^3))$. The space of functions twice differentiable in time taking values in $L^\infty(D,\mathbb{R}^3)$ such that both derivatives belong to $C([0,T_0];L^\infty(D,\mathbb{R}^3))$ is written as $C^2([0,T_0];L^\infty(D,\mathbb{R}^3))$. We now assert the existence and uniqueness for the solution of the initial value problem.

Theorem 3.1 (Existence and uniqueness of the damage evolution) *The initial value problem given by* (2.10) *and* (2.11) *has a solution* $u(x,t)$ *such that for every* $t\in[0,T_0]$, u *takes values in* $L^\infty(D,\mathbb{R}^3)$ *and is the unique solution belonging to the space* $C^2([0,T_0];L^\infty(D,\mathbb{R}^3))$.

Our proof is motivated by recent work [6] where existence of solution for bond based peridynamic models with damage is established. To prove the theorem we will show

(1) The operator $\mathcal{L}^T(u)(x,t)+\mathcal{L}^D(u)(x,t)$ is a map from $C([0,T_0];L^\infty(D,\mathbb{R}^3))$ into itself.
(2) The operator $\mathcal{L}^T(u)(x,t)+\mathcal{L}^D(u)(x,t)$ is Lipschitz continuous with respect to the norm of $C([0,T_0];L^\infty(D,\mathbb{R}^3))$.

The theorem then follows from an application of the Banach fixed point theorem.

To establish properties (1) and (2) we state and prove the following lemmas for the damage factors.

Lemma 3.2 *Let* $H^T(u)(y,x,t)$ *and* $H^D(u)(x,t)$ *be defined as in* (2.8) *and* (2.9). *Then for* $u\in C([0,T_0];L^\infty(D,\mathbb{R}^3))$ *the mappings*

$$(y,x)\mapsto H^T(u)(y,x,t):D\times D\to\mathbb{R},\qquad x\mapsto H^D(u)(x,t):D\to\mathbb{R} \tag{3.1}$$

are measurable for every $t\in[0,T_0]$, *and the mappings*

$$t\mapsto H^T(u)(y,x,t):[0,T_0]\to\mathbb{R},\qquad t\mapsto H^D(u)(x,t):[0,T_0]\to\mathbb{R} \tag{3.2}$$

are continuous for almost all (y,x) *and* x *respectively. Moreover for almost all* $(y,x)\in D\times D$ *and all* $t\in[0,T_0]$ *the map*

$$u\mapsto H^T(u)(y,x,t):C\big([0,T_0];L^\infty\big(D,\mathbb{R}^3\big)\big)\to\mathbb{R} \tag{3.3}$$

is Lipschitz continuous, *and for almost all* $x\in D$ *and all* $t\in[0,T_0]$ *the map*

$$u\mapsto H^D(u)(x,t):C\big([0,T_0];L^\infty\big(D,\mathbb{R}^3\big)\big)\to\mathbb{R} \tag{3.4}$$

is Lipschitz continuous.

Proof The measurability properties are immediate. In what follows constants are generic and apply to the context in which they are used. We establish continuity in time for $H^D(u)$. For $\hat{t}$ and t in $[0,T_0]$ we have

$$\begin{aligned}
&\left|H^D(u)(x,\hat{t})-H^D(u)(x,t)\right|\\
&=\left|h\left(\int_0^{\hat{t}} j_\theta\big(\theta(x,\tau;u)\big)\,d\tau\right)-h\left(\int_0^{t} j_\theta\big(\theta(x,\tau;u)\big)\,d\tau\right)\right|\\
&\le C_1\int_{\min\{\hat{t},t\}}^{\max\{\hat{t},t\}} j_\theta\big(\theta(x,\tau;u)\big)d\tau
\end{aligned}$$

$$\leq \gamma\, C_1 \int_{\min\{\hat{t},t\}}^{\max\{\hat{t},t\}} \left|\theta(x,\tau;u)\right| d\tau$$
$$\leq \gamma\, \ell_1 C_1 C_2 |\hat{t}-t| 2\|u\|_{C([0,T_0];L^\infty(D,\mathbb{R}^3))}. \tag{3.5}$$

The first inequality follows from the Lipschitz continuity of h, the second follows from the growth condition on j_θ, and the third follows from (2.3).

We establish continuity in time for $H^T(u)$. For $\hat{t}$ and t in $[0, T_0]$ we have

$$\begin{aligned}
&\left|H^T(u)(x,\hat{t}) - H^T(u)(x,t)\right| \\
&= \left|h\left(\int_0^{\hat{t}} j_S\big(S(y,x,\tau;u)\big)\, d\tau\right) - h\left(\int_0^{t} j_S\big(S(y,x,\tau;u)\big)\, d\tau\right)\right| \\
&\leq C_1 \int_{\min\{\hat{t},t\}}^{\max\{\hat{t},t\}} j_S\big(S(y,x,\tau;u)\big) d\tau \\
&\leq \gamma\, C_1 \int_{\min\{\hat{t},t\}}^{\max\{\hat{t},t\}} \left|S(y,x,\tau;u)\right| d\tau \\
&\leq \gamma\, C_1 C_2 \frac{|\hat{t}-t|}{|y-x|} 2\|u\|_{C([0,T_0];L^\infty(D,\mathbb{R}^3))}.
\end{aligned} \tag{3.6}$$

The first inequality follows from the Lipschitz continuity of h, the second follows from the growth condition on j_S, and the third follows from the definition of strain (2.1).

To demonstrate Lipschitz continuity for $H^D(u)(x,t)$ we write

$$\begin{aligned}
&\left|H^D(u)(x,t)) - H^D(v)(x,t)\right| \\
&= \left|h\left(\int_0^{t} j_\theta\big(\theta(x,\tau;u)\big)\, d\tau\right) - h\left(\int_0^{t} j_\theta\big(\theta(x,\tau;v)\big)\, d\tau\right)\right| \\
&\leq C_1 \left|\int_0^{t} (j_\theta(\theta(x,\tau;u) - j_\theta\big(\theta(x,\tau;v)\big)\, d\tau\right| \\
&\leq C_1 C_2 \int_0^{t} \left|\theta(x,\tau;u) - \theta(x,\tau;v)\right| d\tau \\
&\leq 2t\ell_1 C_1 C_2 \|u-v\|_{C([0,t];L^\infty(D,\mathbb{R}^3))}.
\end{aligned} \tag{3.7}$$

The first inequality follows from the Lipschitz continuity of h, the second follows from the Lipschitz continuity of j_θ, and the third follows from (2.3). The Lipschitz continuity for $H^S(u)(y,x,t)$ follows from similar arguments using the Lipschitz continuity of h, and j_S, and (2.1), and we get

$$\begin{aligned}
&\left|H^T(u)(y,x,t)) - H^T(v)(y,x,t)\right| \\
&\quad\leq \frac{2tC_1C_2C_3}{|y-x|}\|u-v\|_{C([0,t];L^\infty(D,\mathbb{R}^3))}.
\end{aligned} \tag{3.8}$$

□

Proof of Theorem 3.1 We establish (1) by first noting that

$$\left|\mathcal{L}^T(u)(x,t) + \mathcal{L}^D(u)(x,t)\right| \leq \frac{C}{\delta^2}, \tag{3.9}$$

where C is a constant. This estimate follows from the boundedness of f', g', $H^T(u)$, and $H^D(u)$ and the integrability of the ratios $J^\delta(|y-x|)/|y-x|^2$, $J^\delta(|y-x|)/|y-x|^{3/2}$, and $\omega^\delta(|y-x|)$. Thus $\|\mathcal{L}^T(u)(x,t)+\mathcal{L}^D(u)(x,t)\|_{L^\infty(D,\mathbb{R}^3)}$ is uniformly bounded for all $t\in[0,T_0]$. □

To complete the demonstration of (1) we point out that the force functions $\partial_S f$ and $\partial_\theta g$ are Lipschitz continuous in their arguments. The key features are given in the following lemma.

Lemma 3.3 *Given two functions v and w in $L^\infty(D,\mathbb{R}^3)$ then*

$$\left|\partial_S f\left(\sqrt{|y-x|}S(y,x;v)\right)-\partial_S f\left(\sqrt{|y-x|}S(y,x;w)\right)\right|\le\frac{2C}{\sqrt{|y-x|}}\|v-w\|_{L^\infty(D,\mathbb{R}^3)},\tag{3.10}$$

and

$$\left|\partial_\theta g\big(\theta(x;v)\big)-\partial_\theta g\big(\theta(x;w)\big)\right|\le 2\ell_1 C\|v-w\|_{L^\infty(D,\mathbb{R}^3)}.\tag{3.11}$$

Proof

$$\begin{aligned}&\left|\partial_S f\left(\sqrt{|y-x|}S(y,x;v)\right)-\partial_S f\left(\sqrt{|y-x|}S(y,x;w)\right)\right|\\&\quad\le C\sqrt{|y-x|}\left|S(y,x;v)-S(y,x;w)\right|\le\frac{2C}{\sqrt{|y-x|}}\|v-w\|_{L^\infty(D,\mathbb{R}^3)},\end{aligned}\tag{3.12}$$

where the first inequality follows from the Lipschitz continuity of $\partial_S f$, and the second follows from the definition of S.

For $\partial_\theta g$ we have

$$\left|\partial_\theta g\big(\theta(x;v)\big)-\partial_\theta g\big(\theta(x;w)\big)\right|\le C\left|\theta(x;v)-\theta(x;w)\right|\le 2\ell_1 C_1\|v-w\|_{L^\infty(D,\mathbb{R}^3))},\tag{3.13}$$

where the first inequality follows from the Lipschitz continuity of $\partial_\theta g$, and the second follows from the definitions of θ and S. □

We have

$$\begin{aligned}&\left|\mathcal{L}^T(u)(x,\hat{t})-\mathcal{L}^T(u)(x,t)\right|\\&\quad\le\frac{2}{V_\delta}\int_{D\cap B_\delta(x)}\frac{J^\delta(|y-x|)}{\delta|y-x|}\left|\partial_S f\left(\sqrt{y-x}S(y,x,\hat{t};u)\right)-\partial_S f\left(\sqrt{y-x}S(y,x,t;u)\right)\right|dy\\&\qquad+\frac{2}{V_\delta}\int_{D\cap B_\delta(x)}\frac{J^\delta(|y-x|)}{\delta|y-x|}\left|H^T(u)(y,x,\hat{t})-H^T(u)(y,x,t)\right|dy.\end{aligned}\tag{3.14}$$

From the above, (3.8), and Lemma 3.3 we see that

$$\begin{aligned}&\left\|\mathcal{L}^T(u)(x,\hat{t})-\mathcal{L}^T(u)(x,t)\right\|_{L^\infty(D,\mathbb{R}^3)}\\&\quad\le\frac{\ell_3 C_3}{\delta}\left\|u(x,\hat{t})-u(x,t)\right\|_{L^\infty(D,\mathbb{R}^3)}+\frac{\ell_2\gamma\, C_1C_2}{\delta}|\hat{t}-t|2\|u\|_{C([0,T_0];L^\infty(D,\mathbb{R}^3))}\end{aligned}\tag{3.15}$$

and we see $\mathcal{L}^T$ is well defied and maps $C([0,T_0];L^\infty(D,\mathbb{R}^3))$ into itself.

We show the continuity in time for $\mathcal{L}^D(u)(x,t)$. Now we have

$$\begin{aligned}
&\left|\mathcal{L}^D(u)(x,\hat{t}) - \mathcal{L}^D(u)(x,t)\right| \\
&\quad\le \frac{1}{V_\delta}\int_{D\cap B_\delta(x)} \frac{\omega^\delta(|y-x|)}{\delta^2}\left|\partial_\theta g\big(\theta(y,\hat{t};u)\big) - \partial_\theta g\big(\theta(y,t;u)\big)\right| dy \\
&\qquad + \frac{1}{V_\delta}\int_{D\cap B_\delta(x)} \frac{\omega^\delta(|y-x|)}{\delta^2}\left|H^D(u)(y,\hat{t}) - H^D(u)(y,t)\right| dy \\
&\qquad + \frac{1}{V_\delta}\int_{D\cap B_\delta(x)} \frac{\omega^\delta(|y-x|)}{\delta^2}\left|\partial_\theta g\big(\theta(x,\hat{t};u)\big) - \partial_\theta g\big(\theta(x,t;u)\big)\right| dy \\
&\qquad + \frac{1}{V_\delta}\int_{D\cap B_\delta(x)} \frac{\omega^\delta(|y-x|)}{\delta^2}\left|H^D(u)(x,\hat{t}) - H^D(u)(x,t)\right| dy
\end{aligned} \tag{3.16}$$

and applying Lemma 3.3 and (3.7) to (3.16) we get the continuity

$$\begin{aligned}
&\left|\mathcal{L}^D(u)(x,\hat{t}) - \mathcal{L}^D(u)(x,t)\right| \\
&\quad\le \frac{4\ell_1^2 C_1}{\delta^2}\left\|u(\hat{t},x) - u(t,x)\right\|_{L^\infty(D,\mathbb{R}^3)} + \frac{\gamma\, 4\ell_1^2 C_1 C_2}{\delta^2}|\hat{t}-t|\|u\|_{C([0,T_0];L^\infty(D,\mathbb{R}^3))}.
\end{aligned} \tag{3.17}$$

We conclude that $\mathcal{L}^D$ is well defied and maps $C([0,T_0];L^\infty(D,\mathbb{R}^3))$ into itself and item (1) is proved.

To show Lipschitz continuity consider any two functions u and w belonging to $C([0,T_0];L^\infty(D,\mathbb{R}^3))$, $t\in[0,T_0]$ to write

$$\begin{aligned}
&\left|\mathcal{L}^T(u)(x,t) + \mathcal{L}^D(u)(x,t) - \left[\mathcal{L}^T(w)(x,t) + \mathcal{L}^D(w)(x,t)\right]\right| \\
&\quad\le \frac{2}{V_\delta}\int_{D\cap B_\delta(x)} \frac{J^\delta(|y-x|)}{\delta|y-x|}\Big|\partial_S f\big(\sqrt{|y-x|}S(y,x,t;u)\big) \\
&\qquad - \partial_S f\big(\sqrt{|y-x|}S(y,x,t;w)\big)\Big| dy \\
&\qquad + \frac{2}{V_\delta}\int_{D\cap B_\delta(x)} \frac{J^\delta(|y-x|)}{\delta|y-x|}\left|H^T(u)(y,x,t) - H^T(w)(y,x,t)\right| dy \\
&\qquad + \frac{1}{V_\delta}\int_{D\cap B_\delta(x)} \frac{\omega^\delta(|y-x|)}{\delta^2}\left|\partial_\theta g\big(\theta(y,t;u)\big) - \partial_\theta g\big(\theta(y,t;w)\big)\right| dy \\
&\qquad + \frac{1}{V_\delta}\int_{D\cap B_\delta(x)} \frac{\omega^\delta(|y-x|)}{\delta^2}\left|H^D(u)(y,t) - H^D(w)(y,t)\right| dy \\
&\qquad + \frac{1}{V_\delta}\int_{D\cap B_\delta(x)} \frac{\omega^\delta(|y-x|)}{\delta^2}\left|\partial_\theta g\big(\theta(x,t;u)\big) - \partial_\theta g\big(\theta(x,t;w)\big)\right| dy \\
&\qquad + \frac{1}{V_\delta}\int_{D\cap B_\delta(x)} \frac{\omega^\delta(|y-x|)}{\delta^2}\left|H^D(u)(x,t) - H^D(w)(x,t)\right| dy.
\end{aligned} \tag{3.18}$$

Applying (3.7) and (3.8) to (3.18) delivers the estimate

$$\begin{aligned}&\big\|\mathcal{L}^T(u)(x,t)+\mathcal{L}^D(u)(x,t)-\big[\mathcal{L}^T(w)(x,t)+\mathcal{L}^D(w)(x,t)\big]\big\|_{C([0,t];L^\infty(D,\mathbb{R}^3))}\\&\quad\le\frac{C_1+tC_2}{\delta^2}\|u-w\|_{C([0,t];L^\infty(D,\mathbb{R}^3))},\end{aligned}\tag{3.19}$$

where C_1 and C_2 are constants not depending on time u or w. For $T_0 > t$ we can choose a constant $L > (C_1 + T_0C_2)/\delta^2$ and

$$\begin{aligned}&\big\|\mathcal{L}^T(u)(x,t)+\mathcal{L}^D(u)(x,t)-\big[\mathcal{L}^T(w)(x,t)+\mathcal{L}^D(w)(x,t)\big]\big\|_{C([0,t];L^\infty(D,\mathbb{R}^3))}\\&\quad\le L\|u-w\|_{C([0,t];L^\infty(D,\mathbb{R}^3))},\quad\text{for all } t\in[0,T_0].\end{aligned}\tag{3.20}$$

This proves the Lipschitz continuity and item (2) of the theorem is proved. Note that $u(\tau) = w(\tau)$ for all $\tau \in [0, t]$ implies $\mathcal{L}^T(u)(x,t) + \mathcal{L}^D(u)(x,t) = [\mathcal{L}^T(w)(x,t) + \mathcal{L}^D(w)(x,t)]$ and $\mathcal{L}^T(u)(x,t) + \mathcal{L}^D(u)(x,t)$ is a Volterra operator.

We write evolutions $u(x,t)$ belonging to $C([0,t];L^\infty(D,\mathbb{R}^3))$ as $u(t)$ and $(Vu)(t)$ is the sum

$$(Vu)(t)=\rho^{-1}\big(\mathcal{L}^T(u)(t)+\mathcal{L}^D(u)(t)\big).\tag{3.21}$$

We seek the unique fixed point of $u(t) = (Iu)(t)$ where I maps $C([0,t];L^\infty(D,\mathbb{R}^3))$ into itself and is defined by

$$(Iu)(t)=u_0+tv_0+\int_0^t(t-\tau)(Vu)(\tau)+\rho^{-1}b(\tau)\,d\tau.\tag{3.22}$$

This problem is equivalent to finding the unique solution of the initial value problem given by (2.10) and (2.11). We absorb the factor ρ^{-1} into the Lipschitz constant L and show that I is a contraction map. Observe that the Lipschitz constant diverges as the density goes to zero, i.e.,

$$L\to\infty\quad\text{as }\rho\to 0.\tag{3.23}$$

We now show that I is a contraction map and by virtue of the Banach fixed point theorem we can assert the existence of a fixed point in $C([0,t];L^\infty(D,\mathbb{R}^3))$. To see that I is a contraction map on $C([0,t];L^\infty(D,\mathbb{R}^3))$ we introduce the equivalent norm

$$|||u|||_{C([0,t];L^\infty(D,\mathbb{R}^3))}=\max_{t\in[0,T_0]}\big\{e^{-2LT_0t}\|u\|_{L^\infty(D,\mathbb{R}^3)}\big\},\tag{3.24}$$

and show I is a contraction map with respect to this norm. We apply (3.20) to find for $t \in [0, T_0]$ that

$$\begin{aligned}\big\|(Iu)(t)-(Iw)(t)\big\|_{L^\infty(D,\mathbb{R}^3)}&\le\int_0^t(t-\tau)\big\|(Vu)(\tau)-(Vw)(\tau)\big\|_{L^\infty(D,\mathbb{R}^3)}\,d\tau\\&\le LT_0\int_0^t\|u-w\|_{C([0,\tau];L^\infty(D,\mathbb{R}^3))}\,d\tau\\&\le LT_0\int_0^t\max_{s\in[0,\tau]}\big\{\big\|u(s)-w(s)\big\|_{L^\infty(D,\mathbb{R}^3)}e^{-2LT_0s}\big\}e^{2LT_0\tau}\,d\tau\\&\le\frac{e^{2LT_0t}-1}{2}|||u-w|||_{C([0,T_0];L^\infty(D,\mathbb{R}^3))},\end{aligned}\tag{3.25}$$

and we conclude

$$|||(Iu)(t) - (Iw)(t)|||_{C([0,T_0];L^\infty(D,\mathbb{R}^3))} \le \frac{1}{2}|||u - w|||_{C([0,T_0];L^\infty(D,\mathbb{R}^3))}, \tag{3.26}$$

so I is a contraction map. From the Banach fixed point theorem there is a unique fixed point $u(t)$ belonging to $C([0,T_0];L^\infty(D,\mathbb{R}^3))$ and it is evident from (3.22) that $u(t)$ also belongs to $C^2([0,T_0];L^\infty(D,\mathbb{R}^3))$. This concludes the proof of Theorem 3.1.

4 Energy Balance

The evolution is shown to exhibit a balance of energy at all times. In this section we describe the potential and the energy dissipation rate and show energy balance in rate form. The potential energy at time t for the evolution is denoted by $U(t)$ and is given by

$$U(t) = \frac{2}{V_\delta}\int_D\int_{D\cap B_\delta(x)} \frac{J^\delta(|y-x|)}{\delta} H^T(u)(y,x,t) f\big(\sqrt{|y-x|}S(y,x,t;u)\big)\,dydx + \int_D \frac{1}{\delta^2} H^D(u)(x,t) g\big(\theta(x,t;u)\big)\,dx. \tag{4.1}$$

The energy dissipation rate $\partial_t R(t)$ is

$$\partial_t R(t) = -\frac{2}{V_\delta}\int_D\int_{D\cap B_\delta(x)} \frac{J^\delta(|y-x|)}{\delta} \partial_t H^T(u)(y,x,t) f\big(\sqrt{|y-x|}S(y,x,t;u)\big)\,dydx - \int_D \frac{1}{\delta^2}\partial_t H^D(u)(x,t) g\big(\theta(x,t;u)\big)\,dx. \tag{4.2}$$

The derivatives $\partial_t H^T(u)(y,x,t)$ and $\partial_t H^D(u)(x,t)$ are easily seen to be non-positive and the dissipation rate satisfies $\partial_t R(t) \ge 0$. The kinetic energy is

$$K(t) = \rho\int_D \frac{|\partial_t u(x,t)|^2}{2} dx. \tag{4.3}$$

The energy balance in rate form is given in the following theorem.

Theorem 4.1 *The rate form of energy balance for the damage-fracture evolution is given by*

$$\partial_t K(t) + \partial_t U(t) + \partial_t R(t) = \int_D b(x,t)\cdot\partial_t u(x,t)\,dx. \tag{4.4}$$

Proof of Theorem 4.1 We multiply both sides of the evolution equation (2.10) by $\partial_t u(x,t)$ and integrate over D to get

$$\rho\int_D \partial_t^2 u(x,t)\cdot\partial_t u(x,t)\,dx = \int_D \mathcal{L}^T(u)(x,t)\cdot\partial_t u(x,t)\,dx \tag{4.5}$$

$$+ \int_D \mathcal{L}^D(u)(x,t)\cdot\partial_t u(x,t)\,dx + \int_D b(x,t)\cdot\partial_t u(x,t)\,dx. \tag{4.6}$$

The term on the left side of the equation is immediately recognized as $\partial_t K(t)$. The first and second terms on the right hand side of the equation are given in the following lemma. □

Lemma 4.2 *One has the following integration by parts formulas given by*

$$\int_D \mathcal{L}^T(u)(x,t)\cdot\partial_t u(x,t)\,dx$$
$$= -\frac{2}{V_\delta}\int_D\int_{D\cap B_\delta(x)} \frac{J^\delta(|y-x|)}{\delta} H^T(u)(y,x,t)\partial_t f\big(\sqrt{|y-x|}S(y,x,t;u)\big)\,dydx, \quad (4.7)$$

and

$$\int_D \mathcal{L}^D(u)(x,t)\cdot\partial_t u(x,t)\,dx = -\int_D \frac{1}{\delta^2} H^D(u)(x,t)\partial_t g\big(\theta(x,t;u)\big)\,dx. \quad (4.8)$$

Now note that

$$\partial_t U(t) + \partial_t R(t)$$
$$= \frac{2}{V_\delta}\int_D\int_{D\cap B_\delta(x)} \frac{J^\delta(|y-x|)}{\delta} H^T(u)(y,x,t)\partial_t f\big(\sqrt{|y-x|}S(y,x,t;u)\big)\,dydx$$
$$+ \int_D \frac{1}{\delta^2} H^D(u)(x,t)\partial_t g\big(\theta(x,t;u)\big)\,dx, \quad (4.9)$$

and the energy balance theorem follows from (4.5) and (4.9).

We conclude by proving the integration by parts Lemma 4.2. We start by proving (4.8). We expand $\partial_t g(\theta(x,t))$

$$\partial_t g\big(\theta(x,t;u)\big)$$
$$= \partial_\theta g\big(\theta(x,t;u)\big)\frac{1}{V_\delta}\int_{D\cap B_\delta(x)} \omega^\delta(|y-x|)|y-x|\frac{\partial_t u(y)-\partial_t u(x)}{|y-x|}\cdot e_{y-x}\,dy \quad (4.10)$$

and write

$$-\int_D \frac{1}{\delta^2} H^D(u)(x,t)\partial_t g\big(\theta(x,t;u)\big)\,dx = A(t)+B(t), \quad (4.11)$$

where

$$A(t) = -\int_D \frac{1}{\delta^2} H^D(u)(x,t)\partial_\theta g\big(\theta(x,t;u)\big)\frac{1}{V_\delta}\int_{D\cap B_\delta(x)} \omega^\delta(|y-x|)\partial_t u(y)\cdot e_{y-x}\,dydx \quad (4.12)$$

and

$$B(t) = \int_D \frac{1}{\delta^2} H^D(u)(x,t)\partial_\theta g\big(\theta(x,t;u)\big)\frac{1}{V_\delta}\int_{D\cap B_\delta(x)} \omega^\delta(|y-x|)\partial_t u(x)\cdot e_{y-x}\,dydx. \quad (4.13)$$

Next introduce the characteristic function of D denoted by $\chi_D(x)$ taking the value one inside D and zero outside and together with the properties of $\omega^\delta(|y-x|)$ we rewrite $A(t)$ as

$$A(t) = -\int_{\mathbb{R}^3\times\mathbb{R}^3} \chi_D(x)\chi_D(y)\omega^\delta(|y-x|)\frac{1}{\delta^2}H^D(u)(x,t)\partial_\theta g\big(\theta(x,t;u)\big) \times \frac{1}{V_\delta}\partial_t u(y)\cdot e_{y-x}\,dydx, \tag{4.14}$$

we switch the order of integration and note $-e_{y-x} = e_{x-y}$ to obtain

$$A(t) = \int_D \frac{1}{V_\delta}\int_{D(x)\cap B_\delta(y)} \frac{\omega^\delta(|y-x|)}{\delta^2}H^D(u)(x,t)\partial_\theta g\big(\theta(x,t;u)\big)e_{x-y}\,dx\cdot\partial_t u(y)dy. \tag{4.15}$$

We can move $\partial_t u(x)$ outside the inner integral, regroup factors, and write $B(t)$ as

$$B(t) = \int_D \frac{1}{V_\delta}\int_{D\cap B_\delta(x)} \frac{\omega^\delta(|y-x|)}{\delta^2}H^D(u)(x,t)\partial_\theta g\big(\theta(x,t;u)\big)e_{y-x}\,dy\cdot\partial_t u(x)dx. \tag{4.16}$$

We rename the inner variable of integration y and the outer variable x in (4.15) and add equations (4.15) and (4.16) to get

$$A(t)+B(t) = \int_D \mathcal{L}^D(u)(x,t)\cdot\partial_t u(x,t)\,dx \tag{4.17}$$

and (4.8) is proved.

The steps used to prove (4.7) are similar to the proof of (4.8) so we provide only the key points of its derivation below. We expand $\partial_t f(\sqrt{|y-x|}S)$ to get

$$\partial_t f\big(\sqrt{|y-x|}S(y,x,t;u)\big) = \partial_S f\big(\sqrt{|y-x|}S(y,x,t;u)\big)\frac{\partial_t u(y)-\partial_t u(x)}{|y-x|}\cdot e_{y-x}, \tag{4.18}$$

and write

$$-\frac{2}{V_\delta}\int_D\int_{D\cap B_\delta(x)} \frac{J^\delta(|y-x|)}{\delta}H^T(u)(y,x,t)\partial_t f\big(\sqrt{|y-x|}S(y,x,t;u)\big)\,dydx = A(t)+B(t), \tag{4.19}$$

where

$$A(t) = -\int_D \frac{1}{V_\delta}\int_{D\cap B_\delta(x)} \frac{J^\delta(|y-x|)}{\delta|y-x|}H^T(u)(y,x,t)\partial_S f\big(\sqrt{|y-x|}S(y,x,t;u)\big)\partial_t u(y) \cdot e_{y-x}\,dydx \tag{4.20}$$

and

$$B(t) = \int_D \frac{1}{V_\delta}\int_{D\cap B_\delta(x)} \frac{J^\delta(|y-x|)}{\delta|y-x|}H^T(u)(y,x,t)\partial_S f\big(\sqrt{|y-x|}S(y,x,t;u)\big)\partial_t u(x) \cdot e_{y-x}\,dydx. \tag{4.21}$$

We note that $S(y,x,t;u) = S(x,y,t;u)$ and $H^T(u)(y,x,t) = H^T(u)(x,y,t)$ and proceeding as in the proof of (4.8) we change the order of integration in (4.20) noting that

$-e_{y-x} = e_{x-y}$ to get

$$A(t) = \int_D \frac{1}{V_\delta} \int_{D\cap B_\delta(y)} \frac{J^\delta(|y-x|)}{\delta|y-x|} H^T(u)(x,y,t)\partial_S f\Big(\sqrt{|y-x|}S(x,y,t;u)\Big)e_{x-y}\,dx \cdot \partial_t u(y)\,dy. \tag{4.22}$$

Taking $\partial_t u(x)$ outside the inner integral in (4.21) gives

$$B(t) = \int_D \frac{1}{V_\delta} \int_{D\cap B_\delta(x)} \frac{J^\delta(|y-x|)}{\delta|y-x|} H^T(u)(y,x,t)\partial_S f\Big(\sqrt{|y-x|}S(y,x,t;u)\Big)e_{y-x}\,dy \cdot \partial_t u(x)\,dx. \tag{4.23}$$

We conclude noting that now

$$A(t) + B(t) = \int_D \mathcal{L}^T(u)(x,t) \cdot \partial_t u(x,t)\,dx, \tag{4.24}$$

and (4.7) is proved.

5 Explicit Damage Models, Cyclic Loading and Strain to Failure

In this section we provide concrete examples of the damage functions $H^T(u)(y,x,t)$ and $H^D(u)(x,t)$. We provide an example of cyclic loading and the associated degradation in the nonlocal force-strain law as well as the strain to failure curve for monotonically increasing strains. In this work both damage functions H^T and H^D are given in terms of the function h. Here we give an example of $h(x) : \mathbb{R} \to \mathbb{R}^+$ as follows

$$h(x) = \begin{cases} \bar{h}(x/x_c), & \text{for } x \in (0, x_c), \\ 1, & \text{for } x \le 0, \\ 0, & \text{for } x \ge x_c, \end{cases} \tag{5.1}$$

with $\bar{h} : [0,1] \to \mathbb{R}^+$ is defined as

$$\bar{h}(x) = \exp\left[1 - \frac{1}{1-(x)^a}\right] \tag{5.2}$$

where $a > 1$ is fixed. Clearly, $\bar{h}(0) = 1$, $\bar{h}(1) = 0$, see Fig. 5. Here $h(x)$ increases with x_c.

For a given critical strain $S_c > 0$, we define the threshold function for tensile strain $j_S(x)$ as follows

$$j_S(x) := \begin{cases} \bar{j}(x/S_c), & \forall x \in [S_c, \infty), \\ 0, & \text{otherwise}, \end{cases} \tag{5.3}$$

where $\bar{j} : [1, \infty) \to \mathbb{R}^+$ is given by

$$\bar{j}(x) = \frac{(x-1)^a}{1+x^b} \tag{5.4}$$

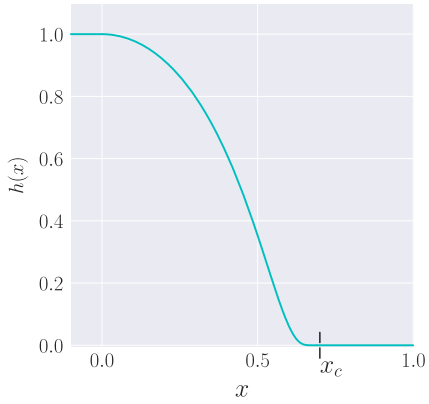

Fig. 5 Plot of $h(x)$ with $a = 2$

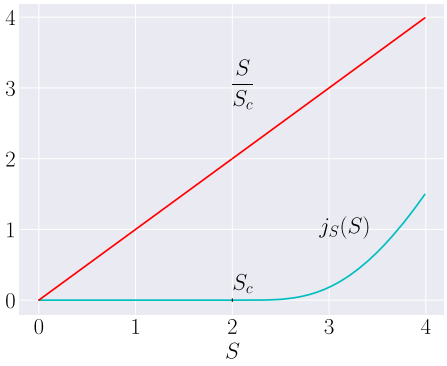

Fig. 6 Plot of $j_S(x)$ with $a = 5$, $b = 5$ and $S_c = 2$

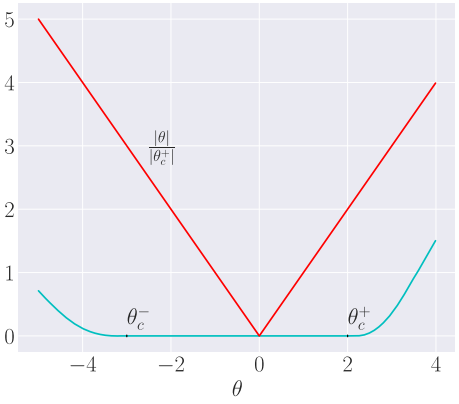

Fig. 7 Plot of $j_\theta(x)$ with $a = 4$, $b = 5$, $\theta_c^+ = 2$, and $\theta_C^- = 3$

with $a > 1$ and $b \geq a - 1$ fixed. Note that $j_S(1) = 0$. Here the condition $b \geq a - 1$ insures the existence of a constant $\gamma > 0$ for which

$$j_S(x) \leq \gamma |x|, \quad \forall x \in \mathbb{R}, \tag{5.5}$$

see Fig. 6.

For a given critical hydrostatic strains $\theta_c^- < 0 < \theta_c^+$ we define the threshold function $j_\theta(x)$ as

$$j_\theta(x) := \begin{cases} \bar{j}(x/\theta_c^+), & \forall x \in [\theta_c^+, \infty), \\ \bar{j}(-x/\theta_c^-), & \forall x \in (-\infty, -\theta_c^-], \\ 0, & \text{otherwise}, \end{cases} \tag{5.6}$$

where $\bar{j}(x)$ is defined by (5.4) and we plot j_θ in Fig. 7. We summarize noting that an explicit form for $H^T(u)(y, x, t)$ is obtained by using (5.1) and (5.3) in (2.8) and an explicit form for $H^D(u)(x, t)$ is obtained by using (5.1) and (5.6) in (2.9).

We first provide an example of cyclic damage incurred by a periodically varying tensile strain. Let x, y be two fixed material points with $|y - x| < \delta$ and let $S(y, x, t; u) = S(t)$ correspond to a temporally periodic strain, see Fig. 8a. Here $S(t)$ periodically takes excursions above the critical strain S_c. During the first period we have

$$S(t) = \begin{cases} t, & \forall t \in [0, S_C + \epsilon], \\ 2(S_C + \epsilon) - t & \forall t \in (S_C + \epsilon, 2(S_c + \epsilon)] \end{cases}$$

and $S(t)$ is extended to $\mathbb{R}^+$ by periodicity, see Fig. 8a. For this damage model we let η be the area under the curve $j_S(x)$ from $x = S_c$ to $x = S_c + \epsilon$. It is given by

$$\eta = \int_{S_c}^{S_c+\epsilon} j_S(x)dx = \int_{t_c}^{t^*} j_S\big(S(t)\big)dt,$$

where t_c corresponds to $S(t_c) = S_c$ and t^* corresponds to $S(t^*) = S_c + \epsilon$. From symmetry the area under the curve $j_S(x)$ under unloading from $S_c + \epsilon$ to S_c is also η. The corresponding damage function $H^T(u)(y, x, t)$ is plotted in Fig. 8b.

In Fig. 9, we plot the strain-force relation where S is the abscissa and the tensile force given by $H^T((u)(y, x, t))\partial_S f(\sqrt{|y - x|}S(y, x, t; u))$ is the ordinate. Here the damage factor $H^T(u)(y, x, t)$ drops in value with each cycle of strain loading. After each cycle, the slope (elasticity) in the linear and recoverable part of the force-strain curve decreases due to damage. The force needed to soften the material is the strength and it is clear from the model that the strength decreases after each cycle due to damage.

Application of this rigorously established model to fatigue is a topic of future research but beyond the scope of this article. We note that fatigue models based on peridynamic bond softening are introduced in [16] and with fatigue crack nucleation in the context of the Paris law in [20].

The next example is strain to failure for a monotonically increasing strain. Here we let $S(y, x, t; u) = S(t) = t$ and plot the corresponding force-strain curve in Fig. 10. We see that the force-strain relation is initially linear until the strain exceeds S_c, the force then reaches its maximum and subsequently softens to failure. At $S^* \approx 0.55025$, we have $\int_0^{S^*} j_S(t)dt = x_c$, and $H^T = 0$. Here we take $\alpha = 1$.

6 Numerical Results

In this section, we conduct numerical simulations to illustrate damage under cyclic loading and monotonic loading. We carry out both examples for two dimensional problems. Let

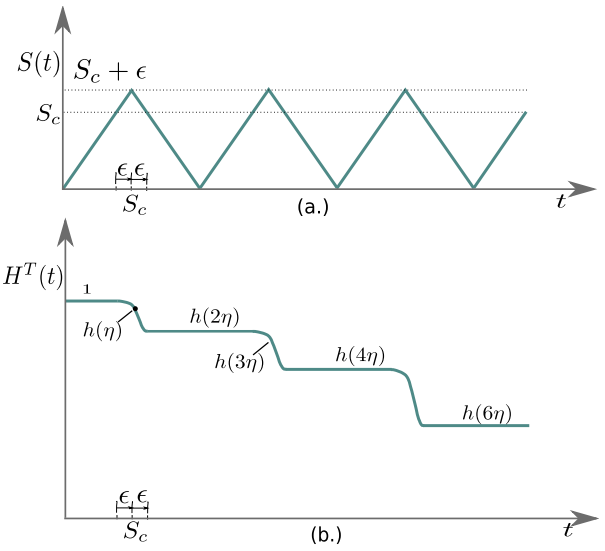

Fig. 8 (**a**) Strain profile. (**b**) Damage function plot corresponding to strain profile

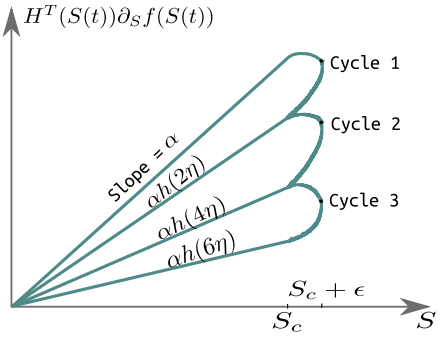

Fig. 9 Cyclic strain vs. Force plot. The initial stiffness is α. Hysteresis is evident in this model

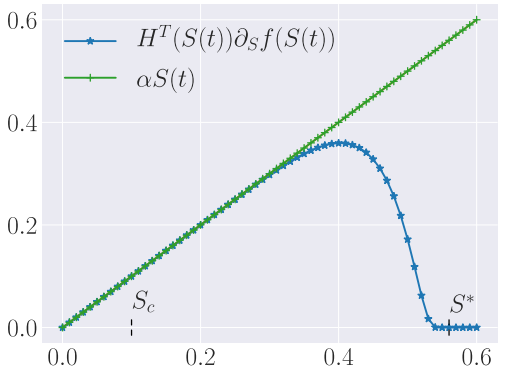

Fig. 10 Strain vs. Force plot where $S(t) = t$. $H^T(S(t))$ begins to drop at $S_c = 0.1$ and $S^* \approx 0.55025$

$x = (x_1, x_2)$ where x_1 corresponds to vector component along the horizontal axis and x_2 corresponds to the component along the vertical axis. Here we use the finite difference ap-

proximation in space together with velocity-verlet scheme in time to generate the numerical results.

We take plane strain quantities given by the Young's modulus $E = 27$ GPa and Poisson's ratio $\nu = 0.2$. The corresponding Lamé modulus is $\lambda = 7.5$ GPa and shear modulus is $\mu = 11.25$ GPa. We apply (7.4) with $J(r) = \omega(r) = 1 - r$, to find $f''(0) = 540.0$ and $g''(0) = -270.0$ and set $r_1 = r_2 = 3.0$ and $r_1^* = r_2^* = 3.0$. This is sufficient to complete the description of the quadratic functions f and g.

We provide values of parameters for the damage functions for which the numerical results in this work and the one presented in [26] Figs. 12.6 and 12.12 show reasonable agreement. For j_S, we let $a = b = 5$ and $S_c = 5 \times 10^{-6}$ and for j_θ, we let $a = 4$, $b = 5$ and $\theta_c^+ = \theta_c^- = 0.01$. The influence function is of the form $J^\delta(r) = \omega^\delta(r) = 1 - r/\delta$ for $0 \le r < \delta$ and zero otherwise. In first numerical example we let $a = 1.01$ and $x_c = 0.6$ for the function h. In second numerical example, we let $a = 2.01$ and $x_c = 0.15$ for the function h. We further remark that higher values of θ_c^+, θ_c^- ensures that damage is only due to bond-based interaction.

6.1 Periodic Loading

Consider a domain $D = [0, 1]^2$ with size of horizon $\delta = 0.15$. The spatial domain is uniformly discretized with mesh size $h = \delta/5$, see Fig. 11. The time domain is $[0, 20]$ seconds and the time step is $\Delta t = 4 \times 10^{-7}$. The density is $\rho = 1200$ kg/m^3. On the top edge, we apply a constant, in x_1, vertical force directed along the x_2 axis. Consider the bond "2" in Fig. 11. We start with zero force and increment the force by $\gamma \Delta t$ every time step until the strain over bond 2 reaches the value $S_{\max} = 0.011 \times 10^{-3}$ (note that bond-strain is dimensionless quantity). Then we start decreasing the force by $\gamma \Delta t$ every time step until the strain of bond "2" is zero. Again, we start incrementing force by $\gamma \Delta t$ until strain reaches $S_{\max}$ and then decreasing force till strain is zero. We continue applying the time periodic force in this way until 20.0 seconds has elapsed. We fix $\gamma = 8861.54$.

The choice of $S_{\max}$ and γ ensures that all bonds near top edge experience strain above S_c for some time in each cycle of loading. Thus, in each cycle, the bond damage increases. In Fig. 12, we plot the time vs. average bond-strain $S(y, x, t; u)$ over bonds 1, 2, and 3 as well time vs. bond-damage $H^T(u)(y, x, t)$ of bond "2". Here, y, x are fixed and correspond to bond "2". In Fig. 13, we plot the bond-force $H^T((u)(y, x, t))\partial_S f(\sqrt{|y - x|}S(y, x, t; u))$ as a function of average strain over bonds 1, 2, and 3. The yellow line is a plot of the undamaged force $\partial_S f(\sqrt{|y - x|}S(y, x, t; u))$ versus strain $S(y, x, t; u)$ curve of bond 2.

6.2 Bending Test

In this example we consider the three-point and four-point bending test considered in Sect. 12.6 of [26]. We consider a slow dynamic evolution by applying a slow monotonic loading. For slow monotone loading, the trends seen in the dynamics are close to the quasistatic case seen in [26]. We consider a beam $D = [0, 1.6] \times [0, 0.25]$ with thickness 0.15 meters and size of horizon $\delta = 0.1$ meters. The mesh size is $h = \delta/4$ meters. The final time is $T = 1$ second and the time step is $\Delta t = 2.0 \times 10^{-6}$.

For the 3 point bending test, illustrated in Fig. 14, we apply displacement boundary conditions at the mesh node $P_{\text{load}} = (0.8, 0.25)$ along the $-x_2$ direction. For the 4-point test, we apply displacement boundary conditions along $-x_2$ direction at two points $P_{\text{load},1} = (0.6, 0.25)$ and $P_{\text{load},2} = (1.0, 0.25)$. For the 3-point test the loading is described by

$$u_2(P_{\text{load}}, t) = -\gamma t, \quad \gamma = 0.001.$$

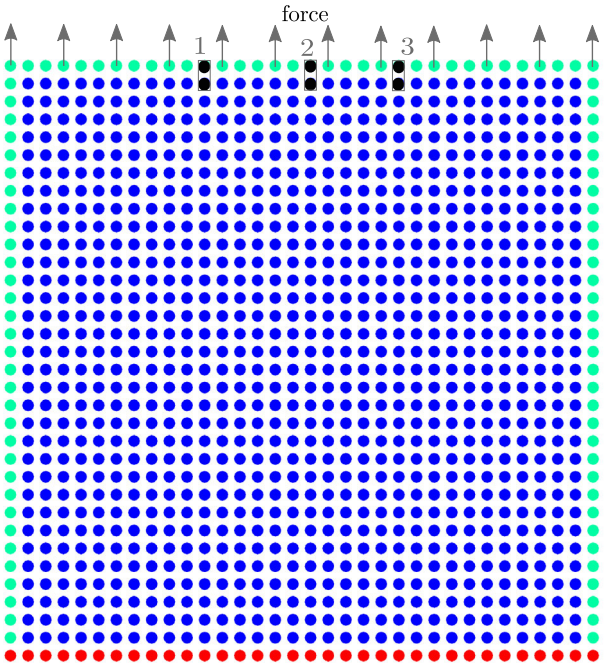

Fig. 11 Discretization of material domain $D = [0, 1]^2$. During simulation we output the bond-strain, bond-force, and damage on bonds numbered as 1, 2, 3. We fix u_1 and u_2 on mesh points colored as Red and fix only u_1 on mesh points colored as green. The same time periodic force is applied to all mesh points on the top edge

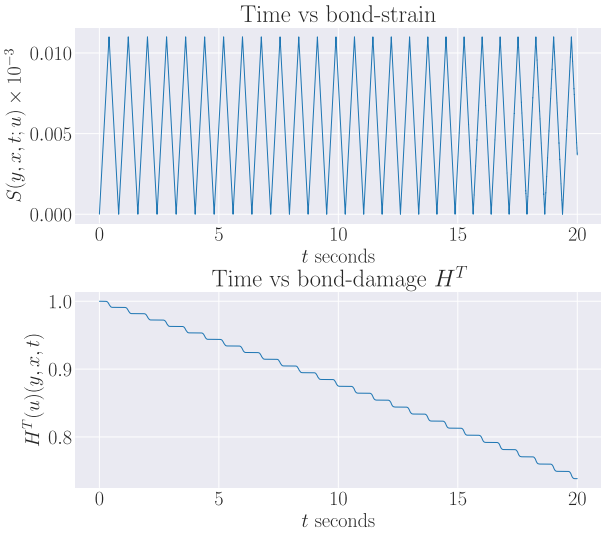

Fig. 12 Time vs. strain $S(y, x, t; u)$ and $H^T(u)(y, x, t)$ plot for bond "2"

Similarly for the 4-point test we have

$$u_2(P_{\text{load},1}, t) = u_2(P_{\text{load},2}, t) = -\gamma t, \quad \gamma = 0.001.$$

In the following figures we plot the deflection of point at the center $(0.8, 0.125)$ of the beam. The force is the total force experienced by mesh node at P_{load} in case of 3-point test and sum of total force experienced by mesh node $P_{\text{load},1}$ and $P_{\text{load},2}$ in case of 4-point test. In Fig. 15,

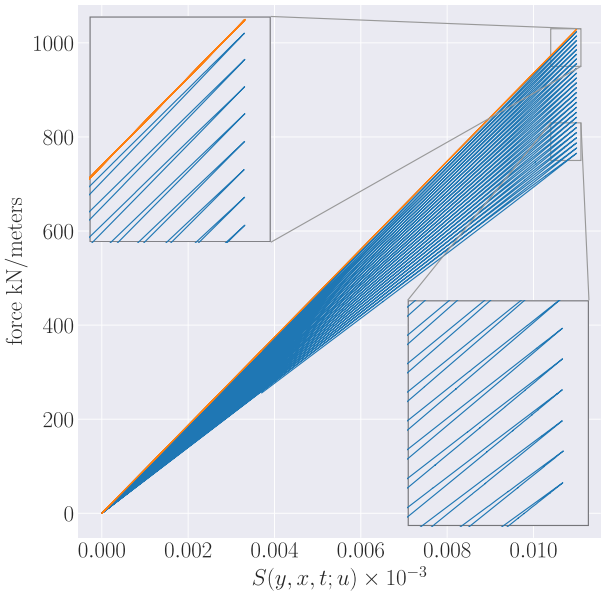

Fig. 13 Strain $S(y,x,t;u)$ vs. force $H^T((u)(y,x,t)) \times \partial_S f(\sqrt{|y-x|}S(y,x,t;u))$ plot averaged over bonds "1, 2, and 3". The yellow line corresponds to $\partial_S f(\sqrt{|y-x|}S(y,x,t;u))$

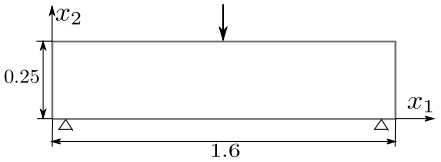

Fig. 14 Schematics of the bending tests. For the 3-point bending test where displacement along $-x_2$ is specified at $(0.8, 0.25)$. At two support points $(0.075, 0.0)$ and $(1.725, 0.0)$, u_2 is fixed. For 4-point bending test, displacement is specified at two points $(0.6, 0.25)$ and $(1.0, 0.25)$

we plot the deflection vs. force curve. If we compare this plot with Fig. 12.6, [26], we find that the results follow the same trend.

The degree of damage about a material point x is given by the damage density $\phi(t,x;u)$. It takes the value $\phi(t,x;u) = 1$ if the point no longer interacts with the surrounding neighborhood, i.e., fully damaged. When there is partial damage one has $0 < \phi(t,x;u) < 1$, and for no damage $\phi(t,x;u) = 0$. Here we damage only for tensile strain as the critical hydrostatic values are taken higher that the critical tensile strain value. For this case the damage density is defined as

$$\phi(t,x;u) = 1 - \frac{\int_{D\cap B_\delta(x)} H^T(u)(y,x,t)dy}{\int_{D\cap B_\delta(x)} dy}. \tag{6.1}$$

We consider the 4 point bending test given by Fig. 16. In Fig. 17 we plot the damage set given by $\phi(t,x;u)$ at the time of structural failure. We see that the highest values of the damage density are highly localized to the vicinity of the applied loads and there is no damage away from the loads.

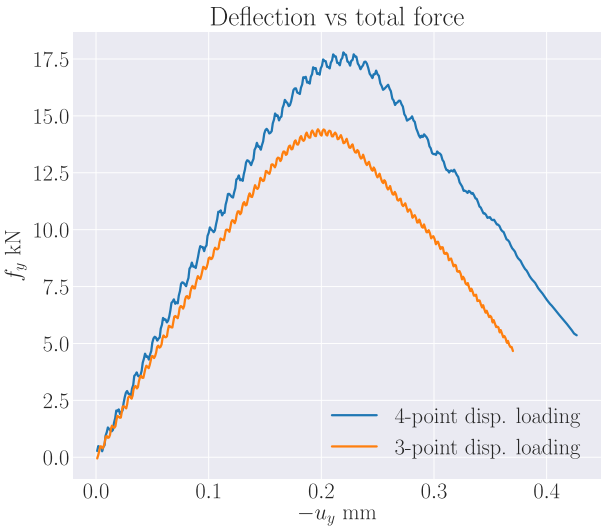

Fig. 15 Deflection vs. force curve. Here we plot the deflection of point at the center $(0.8, 0.125)$ of the beam. The force is the total force experienced by mesh node at P_{load} in case of 3-point test and sum of total force experienced by mesh node $P_{\text{load},1}$ and $P_{\text{load},2}$ in case of 4-point test. The small oscillations seen in the plot are due to the fact that the simulation is dynamic

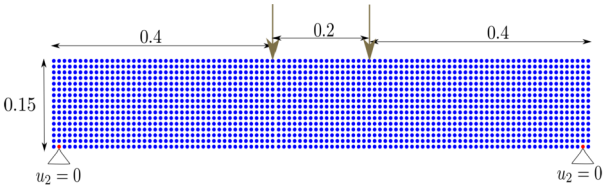

Fig. 16 Schematics of the 4-point bending test where we show damage localization. The displacement along $-x_2$ is specified at the two points $(0.4725, 0.15)$ and $(0.6725, 0.15)$. At two the support points $(0.075, 0.0)$ and $(1.725, 0.0)$, u_2 is fixed

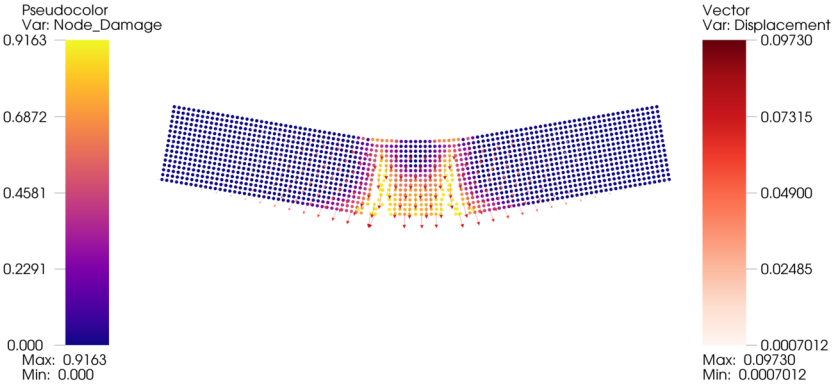

Fig. 17 Damage set. The damage density shows a localization of damage in the vicinity of where the load is applied

7 Linear Elastic Operators in the Small Horizon Limit

In this section we consider smooth evolutions u in space and show that away from damage set the operators $\mathcal{L}^T + \mathcal{L}^D$ acting on u converge to the operator of linear elasticity in the limit of vanishing nonlocality. We denote the damage set by $\tilde{D}$ and consider any open undamaged set D' interior to D with its boundary a finite distance away from the boundary of D and the damage set $\tilde{D}$. In what follows we suppose that the nonlocal horizon δ is smaller than the distance separating the boundary of D' from the boundaries of D and $\tilde{D}$.

Theorem 7.1 *Convergence to linear elastic operators. Suppose that* $u(x,t) \in C^2([0,T_0], C^3(D,\mathbb{R}^3))$ *and no damage, i.e.,* $H^T(y,x,t) = 1$ *and* $H^D(x,t) = 1$, *for every* $x \in D' \subset D \setminus \tilde{D}$, *then there is a constant* $C > 0$ *independent of nonlocal horizon* δ *such that for every* (x,t) *in* $D' \times [0,T_0]$, *one has*

$$\left|\mathcal{L}^T\big(u(t)\big) + \mathcal{L}^D\big(u(t)\big) - \nabla \cdot \mathbb{C}\,\mathcal{E}\big(u(t)\big)\right| < C\delta, \tag{7.1}$$

where the elastic strain is $\mathcal{E}(u) = (\nabla u + (\nabla u)^T)/2$ *and the elastic tensor is isotropic and given by*

$$\mathbb{C}_{ijkl} = 2\mu\left(\frac{\delta_{ik}\delta_{jl} + \delta_{il}\delta_{jk}}{2}\right) + \lambda\delta_{ij}\delta_{kl}, \tag{7.2}$$

with shear modulus μ *and Lamé coefficient* λ *given by*

$$\mu = \frac{f''(0)}{10}\int_0^1 r^3 J(r)\,dr \quad \text{and} \quad \lambda = \mu + g''(0)\left(\int_0^1 r^3 J(r)\,dr\right)^2, \tag{7.3}$$

and for 2 *dimensional problems*

$$\mu = \frac{f''(0)}{8}\int_0^1 r^2 J(r)\,dr \quad \text{and} \quad \lambda = \mu + g''(0)\left(\int_0^1 r^2 J(r)\,dr\right)^2. \tag{7.4}$$

The numbers $f''(0) = \alpha$ *and* $g''(0) = \beta$ *can be chosen independently and can be any pair of real numbers such that* $\mathbb{C}$ *is positive definite.*

Proof We start by showing

$$\left|\mathcal{L}^T\big(u(t)\big) - \frac{f''(0)}{2\omega_3}\int_{B_1(0)} e|\xi|J(|\xi|)e_i e_j e_k\,d\xi\,\partial^2_{jk}u_i(x)\right| < C\delta, \tag{7.5}$$

where $\omega_3 = 4\pi/3$ and $e = e_{y-x}$ are unit vectors on the sphere, here repeated indices indicate summation. To see this recall the formula for $\mathcal{L}^T(u)$ and write $\partial_S f(\sqrt{|y-x|}S) = f'(\sqrt{|y-x|}S)\sqrt{|y-x|}$. Now Taylor expand $f'(\sqrt{|y-x|}S)$ in $\sqrt{|y-x|}S$ and Taylor expand $u(y)$ about x, denoting e_{y-x} by e to find that all odd terms in e integrate to zero and

$$\left|\mathcal{L}^T\big(u(t)\big)_l - \frac{2}{V_\delta}\int_{B_\delta(x)}\frac{J^\delta(|y-x|)}{\delta|y-x|}\frac{f''(0)}{4}|y-x|^2\partial^2_{jk}u_i(x)e_i e_j e_k e_l\,dy\right| < C\delta, \quad l = 1,2,3. \tag{7.6}$$

On changing variables $\xi = (y-x)/\delta$ we recover (7.5). Now we show

$$\left|\mathcal{L}^D\big(u(t)\big)_k - \frac{1}{\omega_3}\int_{B_1(0)} |\xi|\omega(|\xi|)e_i e_j\,d\xi \frac{g''(0)}{\omega_3}\int_{B_1(0)} |\xi|\omega(|\xi|)e_k e_l\,d\xi\,\partial^2_{lj}u_i(x)\right| < C\delta,$$

$$k = 1, 2, 3. \tag{7.7}$$

We note for $x \in D'$ that $D \cap B_\delta(x) = B_\delta(x)$ and the integrand in the second term of (2.6) is odd and the integral vanishes. For the first term in (2.6) we Taylor expand $\partial_\theta g(\theta)$ about $\theta = 0$ and Taylor expand $u(z)$ about y inside $\theta(y,t)$ noting that terms odd in $e = e_{z-y}$ integrate to zero to get

$$\left|\partial_\theta g\big(\theta(y,t)\big) - g''(0)\frac{1}{V_\delta}\int_{B_\delta(y)} \omega^\delta(|z-y|)|z-y|\partial_j u_i(y)e_i e_j\,dz\right| < C\delta^3. \tag{7.8}$$

Now substitution for the approximation to $\partial_\theta g(\theta(y,t))$ in the definition of $\mathcal{L}^D$ gives

$$\left|\mathcal{L}^D(u) - \frac{1}{V_\delta}\int_{B_\delta(x)} \frac{\omega^\delta(|y-x|)}{\delta^2}e_{y-x}\frac{1}{V_\delta}\int_{B_\delta(y)} \omega^\delta(|z-y|)|z-y|g''(0)\partial_j u_i(y)e_i e_j\,dz\,dy\right|$$

$$< C\delta. \tag{7.9}$$

We Taylor expand $\partial_j u_i(y)$ about x, note that odd terms involving tensor products of e_{y-x} vanish when integrated with respect to y in $B_\delta(x)$ and we obtain (7.7).

We now calculate as in ([13] equation (6.64)) to find that

$$\frac{f''(0)}{2\omega_3}\int_{B_1(0)} |\xi|J(|\xi|)e_i e_j e_k e_l\,d\xi\,\partial^2_{jk}u_i(x) = \left(2\mu_1\left(\frac{\delta_{ik}\delta_{jl}+\delta_{il}\delta_{jk}}{2}\right)+\lambda_1\delta_{ij}\delta_{kl}\right)\partial^2_{jk}u_i(x), \tag{7.10}$$

where

$$\mu_1 = \lambda_1 = \frac{f''(0)}{10}\int_0^1 r^3 J(r)\,dr. \tag{7.11}$$

Next observe that a straight forward calculation gives

$$\frac{1}{\omega_3}\int_{B_1(0)} |\xi|\omega(|\xi|)e_i e_j\,d\xi = \delta_{ij}\int_0^1 r^3\omega(r)\,dr, \tag{7.12}$$

and we deduce that

$$\frac{1}{\omega_3}\int_{B_1(0)} |\xi|\omega(|\xi|)e_i e_j\,d\xi\frac{g''(0)}{\omega_3}\int_{B_1(0)} |\xi|\omega(|\xi|)e_k e_l\,d\xi\,\partial^2_{lj}u_i(x)$$

$$= g''(0)\left(\int_0^1 r^3\omega(r)\,dr\right)^2\delta_{ij}\delta_{kl}\partial^2_{lj}u_i(x). \tag{7.13}$$

Theorem 7.1 follows on adding (7.10) and (7.13). The two dimensional calculation follows identical arguments. □

8 Conclusions

We have introduced a simple nonlocal model for free damage propagation in solids. In this model there is only one equation and it describes the dynamics of the displacement using

Newtons law $F = ma$. The damage is a consequence of displacement history and diminishes the force strain law as damage accumulates. The modeling allows for both cyclic damage or brutal damage. The damage is irreversible and the damage set grows with time. The dissipation energy due to damage together with the kinetic and potential energy satisfies energy balance at every instant of the evolution. Future theoretical work will address the question of localization of damage using this model. We believe that if the loading is such that large monotonically increasing strains are generated then damage localization can be anticipated, the numerical examples that we have tried so far support this, see Fig. 17.

In Sect. 6 we presented two numerical examples which illustrate different aspects of the model. The simulations are similar in appearance to Figs. 12.6 and 12.12 of [26]. However the model considered in [26] is distinct from the model presented here and is a time dependent gradient damage model. In that approach one suppresses inertial effects and solves for elastic strains in the form of gradients and time varying damage variables.

In this treatment we have considered dynamic problems with memory. For this case we have shown existence and uniqueness of evolutions for the model. We find that the Lipschitz constant associated with uniqueness goes to infinity as inertial forces go to zero. This is consistent with the loss of uniqueness in the quasi-static limit. The analysis of this model in the absence of inertial forces leads to the quasi-static case where the effects of inertia are absent but a memory of load history is still present. Future work aims to explore this model for this case and understand regimes of body force, specimen geometry and boundary loads for which there is instability and non-uniqueness. The existence of instability and non-uniqueness is well known for quasi-static gradient damage models [17] and appears in the applications [27].

Acknowledgements The authors would like to thank the anonymous referees for their comments.

References

1. Agwai, A., Guven, I., Madenci, E.: Predicting crack propagation with peridynamics: a comparative study. Int. J. Fract. **171**, 65–78 (2011)
2. Bobaru, F., Hu, W.: The meaning, selection, and use of the peridynamic horizon and its relation to crack branching in brittle materials. Int. J. Fract. **176**, 215–222 (2012)
3. Dayal, K., Bhattacharya, K.: Kinetics of phase transformations in the peridynamic formulation of continuum mechanics. J. Mech. Phys. Solids **54**, 1811–1842 (2006)
4. Bobaru, F., Foster, J.T., Geubelle, P.H., Silling, S.A.: Handbook of Peridynamic Modeling. Chapman and Hall/CRC, London (2016)
5. Du, Q., Tao, Y., Tian, X.: A peridynamic model of fracture mechanics with bond-breaking. J. Elast. (2017). https://doi.org/10.1007/s10659-017-9661-2
6. Emmrich, E., Phust, D.: A short note on modeling damage in peridynamics. J. Elast. **123**, 245–252 (2016)
7. Emmrich, E., Weckner, O.: On the well-posedness of the linear peridynamic model and its convergence towards the Navier equation of linear elasticity. Commun. Math. Sci. **5**, 851–864 (2007)
8. Foster, J.T., Silling, S.A., Chen, W.: An energy based failure criterion for use with peridynamic states. Int. J. Multiscale Comput. Eng. **9**, 675–688 (2011)
9. Gerstle, W., Sau, N., Silling, S.: Peridynamic modeling of concrete structures. Nucl. Eng. Des. **237**, 1250–1258 (2007)
10. Ha, Y.D., Bobaru, F.: Studies of dynamic crack propagation and crack branching with peridynamics. Int. J. Fract. **162**, 229–244 (2010)
11. Jha, P.K., Lipton, R.: Numerical analysis of peridynamic models in Hölder space. arXiv:1701.02818 (2017)
12. Lipton, R.: Dynamic brittle fracture as a small horizon limit of peridynamics. J. Elast. **117**, 21–50 (2014)
13. Lipton, R.: Cohesive dynamics and brittle fracture. J. Elast. **124**(2), 143–191 (2016)
14. Lipton, R., Silling, S., Lehoucq, R.: Complex fracture nucleation and evolution with nonlocal elastodynamics. arXiv:1602.00247 (2016)

15. Mengesha, T., Du, Q.: Nonlocal constrained value problems for a linear peridynamic Navier equation. J. Elast. **116**, 27–51 (2014)
16. Oterkus, E., Guven, I., Madenci, E.: Fatigue failure model with peridynamic theory. In: IEEE Intersociety Conference on Thermal and Thermomechanical Phenomena in Electronic Systems (ITherm), Las Vegas, NV, June 2010, 1–6 (2010)
17. Pham, K., Marigo, J.J.: From the onset of damage to rupture: construction of responses with damage localization for a general class of gradient damage models. Contin. Mech. Thermodyn. **25**, 147–171 (2013)
18. Silling, S.A.: Reformulation of elasticity theory for discontinuities and long-range forces. J. Mech. Phys. Solids **48**, 175–209 (2000)
19. Silling, S.A., Askari, E.: A meshfree method based on the peridynamic model of solid mechanics. Comput. Struct. **83**, 1526–1535 (2005)
20. Silling, S.A., Askari, E.: Peridynamic model for fatigue cracking. Sandia Report, **SAND2014–18590** (2014)
21. Silling, S.A., Bobaru, F.: Peridynamic modeling of membranes and fibers. Int. J. Non-Linear Mech. **40**, 395–409 (2005)
22. Silling, S.A., Epton, M., Weckner, O., Xu, J., Askari, E.: Peridynamic states and constitutive modeling. J. Elast. **88**, 151–184 (2007)
23. Silling, S.A., Lehoucq, R.B.: Convergence of peridynamics to classical elasticity theory. J. Elast. **93**, 13–37 (2008)
24. Silling, S., Weckner, O., Askari, E., Bobaru, F.: Crack nucleation in a peridynamic solid. Int. J. Fract. **162**, 219–227 (2010)
25. Weckner, O., Abeyaratne, R.: The effect of long-range forces on the dynamics of a bar. J. Mech. Phys. Solids **53**, 705–728 (2005)
26. Frémond, M.: Non-smooth Thermomechanics. Springer, Berlin (2013)
27. Shao, Y., Zhang, Y., Xu, X., Zhou, Z., Li, W., Liu, B.: Crack patterns in ceramic plates after quenching. J. Am. Ceram. Soc. **94**, 2804 (2001)